Conference on Modelling Fluid Flow (CMFF'22)
The 18th International Conference on Fluid Flow Technologies
Budapest, Hungary, August 30 -September 2, 2022

DEVELOPMENT OF A RADIAL FLOW FAN FAMILY FOR CONTAMINATED GASES OF RELATIVELY HIGH FLOW RATE

Péter Ferenczy[1], Esztella Balla[2], Tamás Benedek[2], Gábor Daku[2], Bálint Kocsis[2], Antal Kónya[1], János Vad[3]

[1] Szellőző Művek Kft. Építész utca 8-12., H-1116 Budapest, Hungary. Tel.: +36 1 204 5972. E-mail: ferenczypeter1@gmail.com
[2] Department of Fluid Mechanics, Faculty of Mechanical Engineering, Budapest University of Technology and Economics.
[3] Corresponding Author. Department of Fluid Mechanics, Faculty of Mechanical Engineering, Budapest University of Technology and Economics. Bertalan Lajos u. 4 – 6, H-1111 Budapest, Hungary. Tel.: +36 1 463 4072, E-mail: vad.janos@gpk.bme.hu

ABSTRACT

The paper outlines the development of a new radial fan family for performing relatively high flow rate for gases laden with solid impurities in technological processes. The paper presents the conceptual preliminary design of the fan family, based on theoretical considerations and empirical guidelines from the literature. The target point of fan design, representing the actual demands by customers on the fan market, was identified on the Cordier diagram. The results of preliminary design have iteratively been refined with involvement of Computational Fluid Dynamics (CFD), the details of which are discussed in the paper, with special regard to flow features being characteristic for this special fan family. The challenging design assignment of finding an aerodynamic compromise between a) the blade geometry customized to the contaminated gas and high specific flow rate, and b) a sufficiently high fan efficiency being in accordance with legislative measures, was successfully solved. A test sample fan was manufactured, and was tested via global measurements. Representative details of the measurements of the fan characteristic and efficiency curves are presented and evaluated in the paper. The potential Industry 4.0 features of the members of the new fan family, being treated as candidates of smart fans operated in smart air technical systems in smart factories, are outlined in the paper.

Keywords:

high specific flow rate, gas with solid contaminants, industrial air technology, radial fan, smart fan

NOMENCLATURE

Latin symbols

A	$[m^2]$	flow cross-section
AR	[-]	aspect ratio of rotor blading
B	$[m]$	fan rotor width (axial extension)
c	$[m/s]$	absolute velocity
D	$[m]$	fan rotor diameter
D_{ref}	$[m]$	reference diameter
N	[-]	rotor blade count
n	$[1/s]$	rotor speed
n_{ref}	$[1/s]$	reference speed
P	$[W]$	useful aerodynamic performance
P_M	$[W]$	shaft input power
Δp_t	$[Pa]$	total pressure rise
qv	$[m^3/s]$	volume flow rate
u	$[m/s]$	circumferential velocity
u_t	$[m/s]$	rotor tip circumferential velocity
v_{ref}	$[m/s]$	reference velocity
t	$[C°]$	gas temperature

Greek symbols

δ	[-]	diameter factor
η	[-]	fan total efficiency
ρ	$[kg/m^3]$	gas density
σ	[-]	speed factor
Φ	[-]	flow coefficient
Ψ	[-]	total pressure coefficient

Subscripts and superscripts

*	blade-passage-averaged data
1	rotor inlet
2	rotor outlet
A	axial flow fan
D	design point
IS	isentropic (ideal, inviscid)
max	maximum
R	radial flow fan
t	rotor blade tip
u	tangential component

1. INTRODUCTION AND OBJECTIVES

The layout of fans is basically customized to demands being specific to the particular industrial applications. Fans applied in industrial air technology and ventilation often serve for fulfilling tasks for which the fluid being transported contains particles of solid contaminants, e.g. dust [1]. The particle-laden flow is usually associated with increased pressure loss in the elements of the air technical system connected to the fan. Furthermore, the system usually incorporates a dust separation equipment, e.g. [2], representing a relatively high pressure loss. In order to cover the demand of relatively high fan pressure rise winning over the aforementioned sources of pronounced pressure drop, the usual type of fan applied for particle-laden gas flows is a *radial flow fan*, e.g. [3].

If the introduction of the solid particles into the fan cannot be avoided for technological reasons, the particles represent a risk of abrasion and deposit formation on the rotor blades and on their surroundings, such as the front and back walls of the rotor. Such risk potentially leads to rotor imbalance as well as deterioration of fan performance and life cycle. As a first-hand guideline for minimizing such unfavourable effects, the flow deflection inside the fan rotor is to be limited. By such means, the inclination of the particles to leave the curved flow paths and to attach on the solid surfaces can be moderated. Radial fan rotors with backward-leaned blades tends to exhibit a moderate flow deflection in comparison to forward-leaned blades. Therefore, *radial fans with rotors of backward-leaned blades*, e.g. [4], tend to be the most widespread in transportation of dusty gas flows, forming the focus of the present paper.

In order to further improve the resistance of the fan against dust load, it is to be emphasized that it is mainly the rotor blades that are exposed to strong effects of abrasion and deposition. Therefore, an appropriate design of rotor blade layout provides a potential for improvement of dust resistance. One principal option to keep mostly away the granular material from the blade surfaces can be carried out by intentional realization of flow separation zones in the vicinity of the blades. A classic example for such layout is when straight, radially aligned blades, e.g. [5-7], are applied in transportation of dusty gas, exhibiting massive flow separation regions within the blade passages. However, flow separation is detrimental from the perspective of the energy efficiency of the fan. Attention is to be drawn to the fact that nowadays' industrial fans are to correspond to the minimum efficiency requirements established in the 327/2011/EU Fan Regulation [8]. Considering only rotors with backward-leaned blades from this point onwards, one possibility for moderating the dust-sensitivity of the blades is to moderate their camber, i.e. to moderate their concavity. By such means, the inclination of the dust to be deposited over the concave blade sections tends to be reduced. Straight, i.e. uncambered backward-leaned blades, e.g. [6], provide a sort of "self-cleaning" geometry, i.e. the developing deposit layer can migrate along the blade chord, and can thus be evacuated from time to time out of the blade passages. However, applying straight blades, instead of curved blades [4, 9-10] of advanced aerodynamic design, tends to be associated with separation of the blade boundary layer, thus deteriorating the efficiency.

Szellőző Művek Kft., termed from this point onwards as Company in the paper, has been engaged in developing a new radial fan family for handling dusty gases with an increased resistance against dust load. This operational requirement has been coupled with demands and orders by industrial customers prescribing a relatively high volume flow rate, as will be illustrated with quantitative data taken from industrial examples. As detailed in the next section, the demand of increased specific flow rate tends to result in preliminary blade design in an increase of the relative outlet width of the rotor, B_2/D_2. Furthermore, in order to adapt the rotor inlet geometry to the increased specific flow rate, a moderation of rotor outer-to-inner diameter ratio D_2/D_1 is to be carried out in preliminary design, resulting in a moderation of the relative blade height $(D_2-D_1)/D_2$ as well. The aforementioned trends suggest that the *aspect ratio* of rotor blading, $AR = [(D_2-D_1)/2]/B_2$ tends to be remarkably reduced. Such moderated AR represents that the outward flow deflection and pressure rise within the rotor, associated with adverse streamwise pressure gradients, is to be realized within a confined space, thus increasing the risk of flow separation over both the front wall of the rotor and along the rotor blades. In order to act against adverse pressure gradients in fluids engineering equipments, e.g. [11], and thus, controlling boundary layer separation for loss reduction, easily adaptable passive flow control techniques, e.g. [12-13], are beneficial.

In order to simultaneously fulfil the aforementioned demands by the industrial customers, being so far uncovered by commercially available products of the Company, the paper presents the outline of developing a new fan family. The new fan product family, termed as LDL fan family, has been developed by the Company in collaboration with the Department of Fluid Mechanics (DFM), Faculty of Mechanical Engineering, Budapest University of Technology and Economics. The multilevel, iterative product development process incorporated preliminary design considerations, Computational Fluid Dynamics (CFD), and prototype testing via global measurements at the premises of the firm. The paper is structured in accordance with these methodological steps. The following work phases were carried out by DFM: preliminary design; design refinements incorporating the evaluation of CFD

results; participation in the experimental tests; evaluation of measurement results.

In lack of any allowances of going into details of long-term and costly basic research, the presented project was dedicated to a robust, cost-effective, and time-effective fulfilment of prescribed practical demands, thus having a new and competitive fan family made available on the market in a relatively short timespan. In this view, the development process demonstrates a *new combination* of *already known*, well-established *methods* in fan design and analysis. From scientific point of view, the objectives of the product development process outlined herein are as follows. These objectives represent the fluids engineering challenges and engineering compromises in simultaneous fulfilment of the following demands, being often contradictory to each other.

- Development of fan rotor blade geometry with backward-leaned, straight plate blades, for increased resistance against dust load, as required by the industrial customers.
- Development of a fan family with increased specific flow rate, i.e. increased design flow coefficient Φ_D, enabling a relatively high volume flow rate even at moderate rotor outlet diameter D_2 and/or rotor speed n, according to the specific industrial demands. By means of limiting D_2, the increase of Φ_D serves for a moderation of space demand and weight of the fan. Furthermore, the limitation of D_2 and/or n results in a reduction of rotor tip circumferential velocity u_t. This is beneficial from the viewpoint of moderating rotordynamic load, and gives also a potential for fan noise reduction, as suggested e.g. by the guideline [14].
- In accordance with the demand of increased Φ_D, development of an aerodynamically effective rotor blade geometry with relatively low *AR*.
- An increased risk of flow separation is foreseen over the blades as well as on the rotor front wall, due to the straight plate blading and relatively low *AR*. Despite such negative tendencies, a reasonably high total efficiency η is to be achieved, in order to guarantee the energy-efficient operation of the fan, and to fulfil the legislative demand manifested in the Fan Regulation [8].
- In solving the contradictory demands outlined above, the *a priori* available passive flow control technology, offered by the unavoidably developing incoming gas jet between the suction cone and the rotor inlet, is to be systematically and purposefully exploited.

The product development process outlined herein resulted in the LDL fan family that has been made available yet on the market. The public technical data presented in the paper are restricted for confidentiality reasons.

2. INDUSTRIAL DEMANDS, AND PRELIMINARY DESIGN CONSIDERATIONS

In what follows, preliminary design considerations are outlined for the radial fan blade layout performing a relatively high volume flow rate, i.e.. high specific flow rate, manifested in a relatively high Φ_D value. For this purpose, axial and radial flow rotors are compared to each other in this section, in a general and comprehensive manner, pointing to the substantial operational differences between the two rotor types. Then, the concept of the radial flow rotor is further developed for obtaining an increased specific flow rate.

As shown in **Figure 1**, comparable axial and radial flow rotors are considered. They are comparable in terms of having identical rotor tip diameters D_t and being driven at identical speed n. Therefore, the rotor tip circumferential velocity u_t is identical. Furthermore, the absorbed power, i.e. the mechanical power input P_M to the rotor shaft, is also taken to be equal. The approximation of identical total efficiencies $\eta = P/P_M$ implies the equality of the useful aerodynamic performance $P = \Delta p_t \cdot q_V$. Representative points in the flow field at rotor inlet (1) and outlet (2) are indicated with cross-symbols in the figure.

For the present comparison, swirl-free inlet to the rotors is assumed. The Euler equation for turbomachines [5, 13, 15-16] reads that the isentropic total pressure rise through the rotor is $\Delta p_{t\,IS} = \rho \cdot u_2 \cdot c_{u2}$. Taking blade-passage-averaged data at the rotor outlet, indicated below with superscript *, Fig. 1 illustrates that the rotor outlet mean circumferential velocity is higher for the radial flow rotor than that for the axial rotor: $u_{2R}^* > u_{2A}^*$; since $u_{2R}^* \equiv u_t$, but $u_{2A}^* < u_t$, taken as an intermediate value between the hub and tip radii of the annulus for the axial rotor. Furthermore, the radial flow rotor blading is capable for performing an increased flow deflection in tangential direction in comparison to the axial flow blading, since the trailing edges of its blades are more inclined toward the circumferential direction (i.e. the trailing edges make a smaller angle with the $\underline{u}$ vector). Considering blade-passage-averaged data again, this yields $c_{u2R}^* > c_{u2A}^*$. Based on the above discussed two inequalities, the Euler equation reads $\Delta p_{t\,IS\,R} > \Delta p_{t\,IS\,A}$. Taking the approximation of equal hydraulic efficiencies for the two rotors, expressing the ratio of $\Delta p_t / \Delta p_{t\,IS}$, the above discussion reflects that *the radial flow rotor tends to perform a higher total pressure rise than the comparable axial rotor:* $\Delta p_{t\,R} > \Delta p_{t\,A}$.

Considering identical useful aerodynamic performances $P = \Delta p_t \cdot q_V$, the condition $\Delta p_{t\,R} > \Delta p_{t\,A}$ implies $q_{V\,R} < q_{V\,A}$, i.e. *the radial flow rotor tends to perform a lower flow rate than the comparable axial rotor*. As Fig. 1 suggests, the particular rotor geometries are adapted to such diverse flow rate-generating capabilities. The entire annulus cross-

section of the axial fan is available for flowing through the blade passages at both inlet and outlet. Contrarily, the inlet cross-section A_{1R} of the radial fan is limited by D_1., and, by such means, $A_{1R} < A_{1A}$. In order to moderate the flow velocity for moderation of the fluid mechanics loss, such limitation of the inlet cross-section is associated with a moderation of the flow rate as well. The outlet cross-section of the radial rotor, determined by the B_2 as well as by the fixed D_2 values, accommodates the design flow rate, in order to ensure an appropriately limited outlet velocity for loss moderation.

The trends discussed above, expressed in the form of equalities and inequalities, are summarized in **Table 1.**

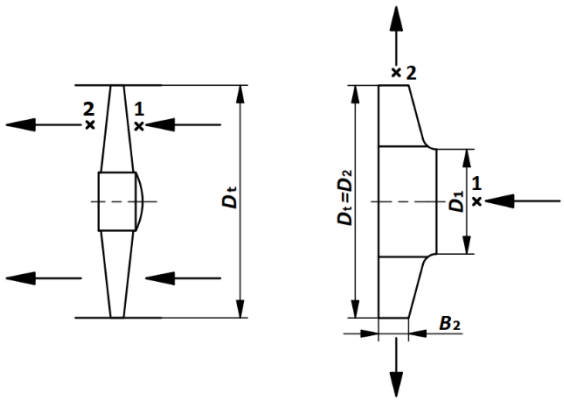

Figure 1. A sketch on comparable axial and radial flow rotors

Table 1. Trends for the comparable axial and radial flow rotors

Axial		**Radial**
D_{2A}	=	D_{2R}
n_A	=	n_R
P_A	=	P_R
u_{2A}*	<	u_{2R}*
c_{u2A}*	<	c_{u2R}*
$\Delta p_{t\,A}$	<	$\Delta p_{t\,R}$
A_{1A}	>	A_{1R}
$q_{v\,A}$	>	$q_{v\,R}$

Table 2. Representative data of market demand survey

q_v [m^3/h]	Δp_t [Pa]	t [$C°$]
$7{,}0\cdot10^3$	400	80
$1{,}0\cdot10^4$	500	35
$2{,}9\cdot10^4$	1000	50
$7{,}5\cdot10^4$	1000	60
$1{,}0\cdot10^5$	1000	170
$1{,}2\cdot10^5$	1600	20
$1{,}5\cdot10^5$	1000	50

As detailed later in this section, the demand by the industrial customers necessitated the increase of the Φ_D value for the radial fan. In order to increase the flow rate delivered by the comparable radial rotor, B_2 is to be increased for increasing the rotor outlet cross-section. This means that the relative outlet width of the rotor B_2/D_2 is to be increased in design. Furthermore, in order to adapt the rotor inlet cross-section to the increased flow rate, D_1 is to be increased, causing a moderation of the relative blade height $(D_2\text{-}D_1)/D_2$. Therefore, for an increased Φ_D, the rotor blades become smaller in height and larger in width, i.e. $AR = [(D_2\text{-}D_1)/2]/B_2$ tends to be reduced. The reduction of AR poses the following challenges: a) The outward flow deflection from the axial inlet toward the radial outlet is to be carried out within an axially extended but radially confined space, thus increasing the risk of boundary layer separation over the rotor front wall. b) Flow turning realized by the rotor blades in tangential direction is to be carried out along radially confined blades, increasing the risk of boundary layer separation along the blades. A purposeful and careful fan design, described in the paper, is to treat the aforementioned challenges.

Table 2 gives an overview of examples for operational data out of a market demand survey, representing demands by potential customers towards the Company. These demands were uncovered by already existing fans of the Company, thus initiating the development of the new fan family presented herein. Therefore, the new fan family aims at extending the operational ranges coverable by the products manufactured by the Company, with a reasonable overlap with the ranges covered by the already existing machines. The datasets are arranged in the sequence of increasing flow rate. They span over more orders of magnitude of flow rate, suggesting the relevance of developing an entire new fan family. Based on the table, a design target was to extend the available product range by a fan family performing up to the order of magnitude of $q_v = 1{,}5\cdot10^5\ m^3/h$, whereas keeping the total pressure rise within the range of Δp_t = 1000-6000 Pa. Further desirable targets were the following. a) Reduced noise and vibration by possibly moderating the rotor tip speed, by means of setting the specific flow rate to an appropriately large Φ_D value. b) Increased resistance against gases laden by dusty or fibrous solid components. To this end, the rotor was instructed by the Company to be designed with backward-leaned straight, i.e. uncambered, plate blades. c) Meeting the efficiency criteria set in the Fan Regulation [8]. Realizing a fairly high efficiency is a design challenge especially in the case of the aforementioned straight rotor blades, in the view that the risk of flow separation is *a priori* increased in the low-AR blades as discussed above. Based on the formulae in [8], a minimum efficiency target of 64 % to 68 % is dictated in the electric input power range

of 10 k*W* to 500 k*W*. Exceeding this efficiency range, achieving at least 70 % maximum efficiency was set as design target, i.e. $\eta_{max} \geq 0{,}70$.

The data in Table 2 enable a classic preliminary design approach [5, 15-16] on the basis of the well-known diameter factor δ and speed factor σ, being in direct relationship with design values of flow coefficient Φ and total pressure coefficient Ψ.

With consideration of gas content as well as pressure and temperature data in Table 2, representative values of ρ can be obtained. Considering each Δp_t data in Table 2 as a fictitious dynamic pressure related to a fictitious reference velocity v_{ref}, such reference velocity can be calculated for each case in Table 2. Considering each qv data in Table 2 as volume flow rate of a fictitious pipe flow at a velocity of v_{ref} through a fictitious circular pipe cross-section $D_{ref}^2 \cdot \pi/4$, the fictitious reference diameter D_{ref} can be calculated for each case. A reference speed n_{ref} can also be obtained for each case, viewing v_{ref} as a fictitious circumferential velocity of solid body rotation at n_{ref} at a fictitious radius of $D_{ref}/2$, i.e. $v_{ref} = D_{ref} \cdot \pi \cdot n_{ref}$.

The ratio between the true rotor outlet diameter and the reference diameter is the diameter factor δ. The ratio between the true rotor speed and the reference speed is the speed factor σ.

$$\delta = D_2 / D_{ref} \quad (1)$$

$$\sigma = n / n_{ref} \quad (2)$$

Once relevant empirical data are obtained for δ and σ, the D_2 and n characteristics being necessary for realizing the operational data in Table 2 can therefore be calculated for each case of specific market demand. The Cordier diagram [5, 15, 17] presents empirical [δ, σ] data couples for fans realizing reasonably high efficiency. According to the long-term experiences gathered at DFM in industrial fan design, the following approximate ranges and correlations are valid for δ and σ for high-efficiency radial fans with backward-leaned blades:

$$2 \leq \delta \leq 4 \quad (3)$$

$$\sigma = 1 / \delta \quad (4)$$

A direct relationship exists between the [δ, σ] and [Φ, Ψ] data couples enabling high-efficiency operation. Considering the definitions of the flow and total pressure coefficients,

$$\Phi = q\text{v} / [(D_2^2 \cdot \pi/4) \cdot u_t] \quad (5)$$

$$\Psi = \Delta p_t / (\rho \cdot u_t^2/2) \quad (6)$$

and substituting $u_t = D_2 \cdot \pi \cdot n$, the following relationships can be obtained [5, 15]:

$$\delta = \Psi^{0,25} \cdot \Phi^{-0,5} \quad (7)$$

$$\sigma = \Phi^{0,5} \cdot \Psi^{-0,75} \quad (8)$$

By taking Eqs. (3) to (8) into account, the following approximate ranges and values of dimensionless operational coefficients are characteristic for high-efficiency radial fans with backward-leaned blades: $\Phi = 0{,}06 \ldots 0{,}25$; $\Psi = 1{,}0$.

Intermediate calculations were carried out for the cases in Table 2, in order to establish preliminary design values of [δ, σ] as well as [Φ, Ψ] for the new fan family. During these calculations, the following requirement were taken into consideration. a) The obtained D_2 values are to fit to the Rénard series of usual rotor diameters [18-19]. b) The necessary rotor speed n is to be realizable by usually available means, i.e. either by direct drive using an asynchronous electric motor, or by using a direct-driven asynchronous motor equipped with a frequency converter, or by using a V-belt indirect drive. Such intermediate calculations resulted in the following compromise in the preliminary design phase: $\delta_D = 2{,}36$; $\sigma_D = 0{,}42$; $\Phi_D = 0{,}18$; $\Psi_D = 1{,}0$. **Figure 2** illustrates the Cordier diagram, e.g. [5, 7, 15, 17], and position of the design [δ, σ] data couple of the new fan family in the diagram. Representative zones for various types of turbomachines – not necessarily covering the entire range of validity in the figure – are indicated with grey regions. As the diagram reflects, the new fan family is characterised by relatively small δ_D as well as by relatively large σ_D values. It is located at the boundary of the radial fan range, forming a sort of transition towards the group of mixed-flow fans, usually characterized by higher Φ_D and lower Ψ_D than radial machines. Indeed, the diameter factor $\delta_D = 2{,}36$ is in the vicinity of the lower threshold of the usual radial fan range of $2 \leq \delta \leq 4$, corresponding to a relatively high flow coefficient $\Phi_D = 0{,}18$ within the usual range of $\Phi = 0{,}06 \ldots 0{,}25$; thus corresponding to the industrial demand of increased specific flow rate, as discussed previously in the paper.

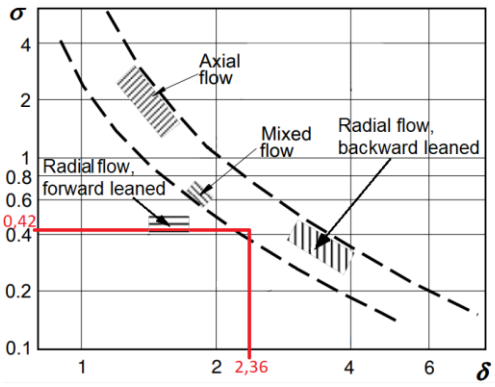

Figure 2. Cordier diagram, reproduced from [7], indicating the design point of the new fan family

3. FAN DESIGN AND DEVELOPMENT

The preliminary design of each component of the new fan family – i.e. suction and pressure ducts, inlet cone, rotor with front and back walls enclosing the blades, and scroll casing – was carried out in line with the recommendations originating from the classic literature [5, 15-16], considering the basic fluid mechanics principles and turbomachinery laws documented in references [13, 20]. The design guidelines and drawings of the already existing LDH fan family of the Company, proven to be successful on the market, were taken as a reference and starting point. Examples for the literature-based preliminary design guidelines are as follows – considering that publication of quantitative data is restricted, due to confidentiality reasons.

N = 12 rotor blades have been designed, in accordance with the guidelines formulated by Bommes in [15]. Although such blade count appears to be relatively high for rotors with backward-leaned blades, the relatively high blade solidity associated with the high blade count tends to exhibit the advantage of moderating the flow separation within the blade passages; thus improving the efficiency.

In the rotating frame of reference of the rotor, the angle of rotor-inlet flow with respect to the circumferential direction has been determined with consideration of the displacement effect caused by the blades. Relative to this inflow direction, the inlet metal angle of the rotor blades was increased by empirical means for improving the dust-resistance of the blading, following the recommendation in Reference [15] after Bommes.

According to the guidelines for designing high-efficiency radial fans in [5, 15], the diameter ratio D_2/D_1 was set between 1,3 and 2; taking into account that higher design flow coefficient Φ_D tends to reduce the diameter ratio, as was qualitatively explained in Sections 1 and 2.

The blade outlet metal angle – relative to the circumferential direction – and the chord length of the blades, being results of the prescribed inlet metal angle and the D_2/D_1 ratio for the backward-leaned straight blades, have been in accordance with the recommendations by Bommes and Eck [5, 15].

In order to assess the appropriateness of the preliminarily designed fan geometry, and to realize sensitivity studies on setting the geometrical parameters, CFD computations were carried out. The simulations were elaborated in ANSYS Fluent® software environment, using the frozen rotor model, e.g. [3-4], in order to rationalize the cost of CFD, in terms of both computational time and utilization of computational capacity, for the multiple CFD runs applied. The applicability of the frozen rotor approach has been confirmed via making a comparison with a moving-mesh model in a representative scenario. A fair agreement has been experienced between the results obtained using the frozen rotor model and the moving-mesh model.

The effect of turbulent phenomena was taken into account using the SST k-ω model, commonly used in the simulation of rotating machines, e.g. [3, 7]. The accuracy of this turbulence model is increased by improving the spatial resolution of the boundary layer along the walls. Therefore, special care was taken in keeping the first near-wall cells sufficiently small over the critical solid surfaces, such as the rotor blades, the rotor front wall, and the rotor back wall. Hexahedron elements were used for the mesh, enabling a fair spatial resolution using a relatively low number of cells. Nearly 15 million cells were used in the overall model, judged to be adequate, as grid dependence studies revealed. The CFD models were validated to global measurement data on the commercially available LDH fan family, for which the applied CFD methodology has been adopted in representative validation scenarios.

In what follows, a few representative CFD scenarios and results are discussed qualitatively in exemplary case studies. The geometries presented in the CFD results represent intermediate phases of the development, i.e. they differ from the finalized geometry, due to confidentiality reasons.

Applying uncambered, i.e. straight rotor blades, as well as having a reduced AR for the rotor blading, represent simultaneous challenges from the design perspective of moderating flow separation within the rotor, in order to achieve a reasonably high efficiency, conf. [8]. Therefore, the primary goal of the CFD campaign was to identify separated flow regions, and to elaborate remedial strategies against them. The effect of straight blades is discussed first. The originally blunt leading and trailing edges of the plate (sheet metal) blades were appropriately profiled, as a compulsory practice in moderation of separation from the blades. In accordance with the literature, e.g. [5], the CFD studies confirmed the development of separation zones on the suction side of the blades, due to the straight blade geometry. The blockage effect due to these flow separation zones causes a non-uniform, jet-like rotor exit flow, resulting in the increase of rotor exit loss, approximated as loss of a Borda-Carnot type sudden expansion [11, 13] from the jet-like rotor exit flow cross-sections to the scroll casing. The CFD runs justified that increasing the blade solidity caused a suppression of the interblade flow separation, and thus led to efficiency improvement, predominantly by reducing the Borda-Carnot type loss. By such means, the appropriateness of the preliminarily set blade count of N = 12 has been confirmed. Reducing the blade count relative to this design value would result in a deterioration of the efficiency, as CFD sensitivity studies pointed out. In addition to choosing the adequate blade count, a suitable fine-adjustment of the blade angle was carried out. On this basis, flow separation from the blade surfaces has significantly been reduced. **Figure 3** shows an example for the radial velocity distribution within the

rotor, for a representative intermediate development phase of the fan. The CFD example is related to D_t = 1,60 *m*; n = 950 1/*min*; u_t = 79,6 *m*/*s*; design flow rate. In the figure, zones of negative radial velocity are indicators of reverse flow within the regions of flow separation. One of such reverse flow zones is labelled in the figure for illustration. As the figure suggests, flow separation from the blades is an *inevitable* consequence of applying straight blades; however, the CFD-aided careful design process resulted in a significant suppression of such separation.

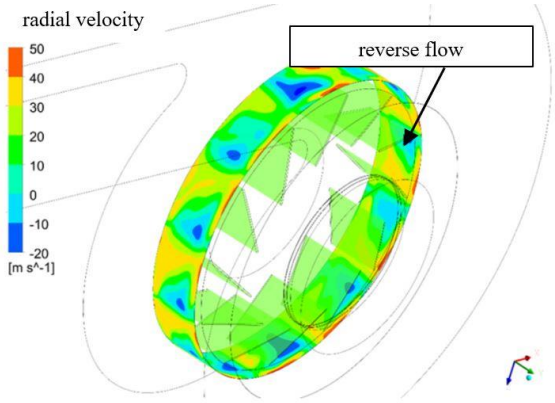

Figure 3. CFD representation of radial velocity within the rotor: an example.

During preliminary design, the geometry of the suction cone, as well as the geometry of the front wall of the rotor was prescribed following the guidelines in the literature [5, 15-16]. The preliminary design incorporated selection and harmonization of rounding radii applied to the suction cone and to the rotor inlet section. Even by setting such suction cone and front wall geometry, considered as favourable by empirical means, the CFD analyses revealed a separation zone over the conical front wall of the rotor, due to the relatively low blade *AR*, corresponding to a drastic outward flow deflection within the front region of the rotor. A high-loss zone was also recognized during the CFD campaign in the zone close downstream of the fitting between the suction cone and the rotor, for certan geometrical varieties. Another consequence of increased rotor width is the non-uniformity of velocity inlet to the blading, as indicated by the CFD studies. As remedial strategy against all of the aforementioned adverse effects, the concept of passive boundar layer control was selected, utilizing the *a priori* and inevitably occurring leakage flow between the suction cone and the rotor front wall. Such leakage flow develops from the high-pressure zone of rotor outlet toward the gap between the suction cone and the rotor front wall, within the scroll casing, and therefore, is primarily the adverse manifestation of volumetric loss. However, such leakage flow, appearing in the form of a concentrated high-momentum jet incoming at the periphery of the rotor inlet, may be exploited for energizing the boundary layer, thus moderating the extension of flow separation, and promoting flow reattachment [13]. The efficiency-increasing benefit of such boundary layer control may significantly dominate over the efficiency-reducing effect of volumetric loss.

According to the above, the geometry and size of the gap between the suction cone and the front wall of the rotor was treated with special care. In preliminary design of the gap geometry, the empirical correlations available in the literature [5] between the available maximum fan efficiency and the gap-to-D_2 size ratio were considered. After preliminary design, the geometrical arrangement and size of the gap were refined via CFD-aided campaigns. **Figures 4 and 5** provide two CFD examples for tested intermediate geometries of gap layouts during the development process. The conditions of investigation are as written for Fig. 3. Fig. 4 is an example in which the suction cone outlet and the rotor inlet are coaxial cylindrical surfaces, and a radial gap is set in between them. The figure indicates a boundary layer separation zone over the introductory section of the divergent part of the rotor front wall. Such separation zone extends also into the blading. The above suggest that the incoming leakage flow was unable to significantly contributing to remediating such separation phenomenon. Fig. 5 presents another example for the CFD-aided gap design, in an intermediate development phase. Here, the rotor suction cone represents a convergent-divergent cross-section, and the gap between the suction cone and the rotor front wall has been shifted to the outlet of the divergent section of the suction cone, fitting to the nearly conical front wall of the rotor. In this case, the incoming sloped leakage flow tends to eliminate fully the flow separation over the suction cone; the separating region is confined to the front part of the rotor blading.

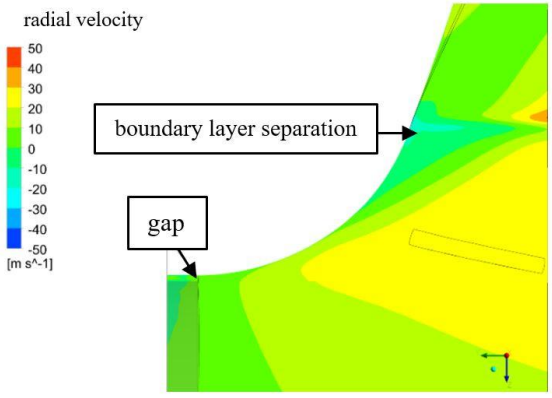

Figure 4. An example for a CFD test on a radial gap between the suction cone and the rotor front wall. Part of the meridional section. Radial velocity distribution.

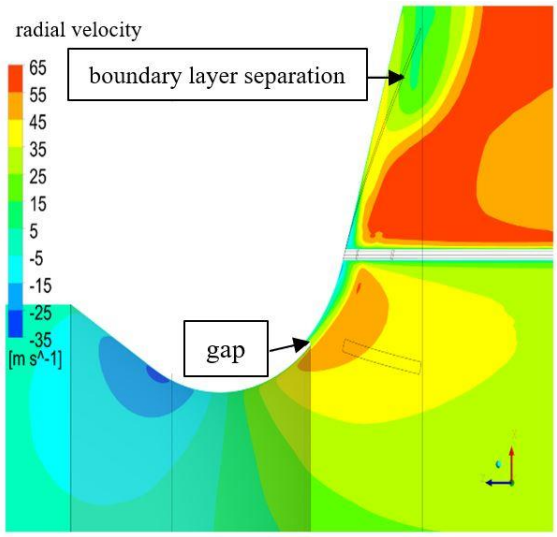

Figure 5. An example for a CFD test on a modified inlet and gap geometry. Part of the meridional section. Radial velocity distribution.

The CFD-aided design of the gap was a challenge in realizing a compromise between the following trends. a) The gap is to be reasonably small for enabling a sufficiently high volumetric efficiency. b) The gap is not be too small, in order to avoid the necessity for excessive strictness of manufacturing tolerances, and to guarantee an easy assembly process. c) The gap is to be sufficiently large, and the geometrical arrangement of the gap (i.e. gap direction) is to be chosen adequately, in order to maintain an appropriate incoming leakage flow for refreshing the boundary layer. Determining a suitable gap size and geometry, and finalizing the rounding radii applied to the suction cone and to the rotor inlet section, were subject to CFD campaigns. The edges of the suction cone and the rotor inlet, made of sheet metal, were also treated appropriately, in order to further moderate flow separation.

4. MANUFACTURING AND TESTING OF A REPRESENTATIVE FAN

Based on the design process outlined above, a representative test sample of the new LDL fan family was manufactured. The test sample, corresponding to the fan of type identifier of LDL-k63, has the following characteristics: D_2 = 630 *mm*, nominal rotor speed n = 1470 1/*min*, direct-driven by an 11 k*W* 4-pole asynchronous electric motor. The photograph of the fan is shown in **Figure 6**.

The aim of manufacturing the test fan was to experimentally justify the success of the design process, to examine the aerodynamic characteristics of the fan via global measurements, and, on this basis, to establish an initial empirical basis for characteristic and efficiency curves to be incorporated in the commercial documentation of the new fan family. For the global measurements, a test facility was realized at the premises of the Company, with consideration of the guidelines documented in standard [21]. The test rig selected by the Company is a type "C" [21] ducted-inlet, free-outlet configuration. In accordance with [8], such facility is primarily assigned to determining the static pressure rise as well as static efficiency. In addition, with knowledge of the gas density, volume flow rate, and cross-section of the pressure-side port of the fan, the outlet dynamic pressure can be approximated, and thus, estimation can be given to the total pressure rise Δp_t and total efficiency η , as presented in this paper. The flow rate was measured in the inlet duct using a throughflow orifice plate, with consideration of standards [22-23]. The following relative errors were estimated conservatively as representative mean values over the actual measurement ranges for the quantities playing role in the experiments. These errors meet the instructions for the maximum allowable uncertainties in [21]. Barometric pressure: ± 0,2 %. Absolute temperatures: ± 0,2 %. Electric input power to the driving motor: ± 2,0 %. Static pressure upstream of the orifice plate, relative to atmospheric; pressure difference on the orifice plate; depression upstream of the fan, relative to the atmospheric pressure: max. ± 0,2 %. Pressure rise: ± 0,4 %. Volume flow rate: ± 1,5 %. Rotor speed: ± 0,2 %. Carrying out an error propagation analysis with consideration of the guidelines in [21-23], taking the „root-mean-square" propagation concept for the relative errors into account (examples e.g. in [21-22]), the following absolute uncertainties have been estimated for the dimensionless global characteristics presented in the paper. These absolute uncertainties are valid at 95 % confidence level for the operational range of $\Phi = 0{,}1 \ldots 0{,}18$ fulfilling the design criterion of $\eta \geq 0.70$. Absolute errors: for Φ: ± 0,003; for Ψ: ± 0,01; for η: ± 0,03.

Figure 6. Photograph of the LDL test fan

Figures 7 and 8 present the measurement-based dimensionless characteristic and efficiency curves. In the figures, 4th order polinomials have been fitted to the data points, by means of the least-squares method.

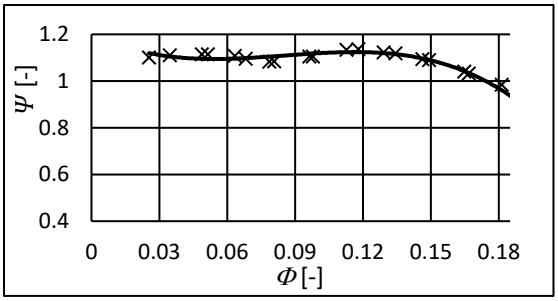

Figure 7. Measurement-based dimensionless $\Psi(\Phi)$ characteristic curve

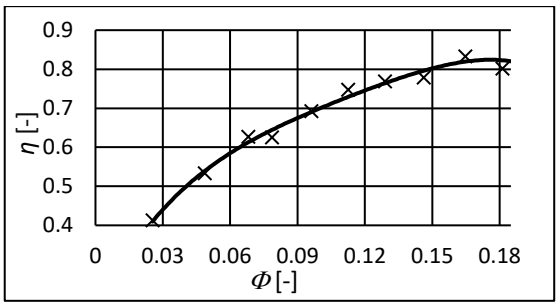

Figure 8. Measurement-based dimensionless $\eta(\Phi)$ efficiency curve

The curves presented in this paper indicate an upper limit of the measurements at $\Phi = 0{,}18$. Such limitation is predominantly due to the throttling effect of the orifice plate, in absence of a booster fan. Since an especial interest is to apply these fans at increased specific flow rates, the measurement methodology was necessary to be extended toward higher Φ values, as will be discussed in a future paper. The characteristic and efficiency curves justify the appropriateness of the design method, from the following perspectives. At the design flow rate of $\Phi_D = 0{,}18$, the fan fairly well realizes the designed total pressure rise of $\Psi_D = 1{,}0$. The maximum of the efficiency curve is related to the design point at $\Phi_D = 0{,}18$, indicating that the design process was successful also in terms of energy efficiency, i.e. the design point is also regarded as the best efficiency point. The obtained maximum efficiency is significantly higher than the set minimum design target of $\eta_{max} \geq 0{,}70$. The operational range of $0.12 \leq \Phi \leq 0.18$ exhibits Ψ values continuously decreasing with Φ, ensuring stable operation. In this range, the efficiency values are fairly above $\eta = 0{,}70$, thus guaranteeing energy-efficient operation, and meeting the Fan Regulation [8] with a reassuring safety reserve.

Standard [24] specifies tolerance grades, to be guaranteed by the fan manufacturer for its products, with regard to assigned nominal values of the volume flow rate, pressure rise, efficiency, and absorbed power. **Table 3** gives an overview of the tolerance grades, according to [24]. The tolerance is negative for the efficiency, and is positive for the absorbed power; meaning that an efficiency deterioration and power input increase is accepted – provided that the fan also meets the tolerances specified for the volume flow rate and pressure rise. If sheet material is applied in fan manufacturing, with surface protection, the standard *a priori* assigns the expectable tolerance grade of AN4 to the products. In the case of sheet material with special surface protection enabling increased geometrical accuracy – e.g. hot dip galvanizing –, the tolerance grade AN3 is also achievable [24]. Since the Company manufactures its fans from sheet metal parts, the tolerance grade AN4 is routine, or the stricter tolerance grade AN3 may also be ambitioned in the case of the new LDL fan family. This fits also to the fact that the standard [24] assigns the tolerance grades AN4 and AN3 to e.g. industrial fans operated in process engineering under harsh (abrasive or corrosive) circumstances.

If the measurements carried out on the test sample fan are to be used for generation of the commercial documentation of the LDL fan family, using the fan scaling laws [5, 15-16], the following considerations are to be made when determining the reportable tolerance grades. a) Measurement errors, as reported above. b) Reynolds number effects, affecting the accuracy of scaling laws. c) Manufacturing tolerances. Considering the reported measurement errors, the Reynolds number effects, and the manufacturing tolerances being usual in the practice of the Company, the AN4 tolerance grade is feasible as routine for the LDL family. For special requirements, necessitating more strict manufacturing tolerances, the AN3 grade is also achievable, upon demand by the customer. It is noted herein that the strategy of the Company is striving to satisfy the customers' needs by allowing for only positive tolerances for the volume flow rate and pressure, i.e. overestimating the nominal duty point in an optimistic approach, within the specified ranges in the tolerance grade under consideration.

Table 3. Tolerance grades and tolerance boundaries, in accordance with standard [24]

Quantity	Tolerance grade			
	AN1	AN2	AN3	AN4
Flow rate	±1 %	±2,5 %	±5 %	±10%
Pressure rise	±1 %	±2,5 %	±5 %	±10%
Efficiency	-1%	-2%	-5%	-12%
Power	+2%	+3%	+8%	+16%

In future applications of the fans manufactured by the Company, the Industry 4.0 perspectives may gather an increased importance, in the view that smart factories may incorporate smart industrial air technology and smart ventilation. Such systems are

to be served by smart fans. Among others, as described in [25], the smart features of a fan incorporate smart condition monitoring, self-diagnostics and intelligent maintenance against contamination and erosion, e.g. via vibration and acoustics measurements. As outlined in [25], members of the new LDL fan family can be regarded as candidates for implementing such smart features, being in accordance with the vision by the Company. The importance of smart condition monitoring for the LDL family, coupled with smart operation and maintenance, is emphasized by the fact that the solid contaminants may cause erosion or deposit on the fan components, and such negative effects can be monitored e.g. via on-line vibration diagnostics.

5. SUMMARY

Szellőző Művek Kft., in collaboration with the Department of Fluid Mechanics, Faculty of Mechanical Engineering, Budapest University of Technology and Economics, have developed a new radial flow fan family for increased specific flow rate for transporting gases laden with solid contaminants. The new fan family, labelled as LDL fans, is equipped with backward-leaned straight plate blades, for increased resistance against blade erosion or deposit formation. The relatively large specific flow rate prescribed in the design process necessitated the development of a rotor with moderate outlet-to-inlet diameter ratio, and moderate aspect ratio. The preliminary design of the fan family was carried out on the basis of literature recommendations. The design challenges posed by the simultaneous risk of separation zones over the blade suction sides and over the front wall of the rotor necessitated the application of CFD-aided careful iterative refinement of the fan geometry, in order to moderate the separation regions. As a remedial strategy against flow separation, a passive flow control method was elaborated by purposefully exploiting the incoming leakage flow in the gap between the suction cone and the rotor inlet for energizing the boundary layers in the critical flow regions. A test sample was manufactured and tested via global measurements. The experiments revealed the appropriateness of the design method, in terms of achieving the target design point, and enabling a fairly high efficiency, being in accordance with the Fan Regulation [8]. Experimental testing, together with manufacturing considerations, enables the accordance of the new LDL fan family to the AN4 or even AN3 tolerance grades [24]. Corresponding to the vision by the Company, the new fan family is a potential candidate for adapting smart fan features, e.g. intelligent condition monitoring and maintenance, against blade erosion or contaminant deposit, in line with the Industry 4.0 perspective [25]. Thanks to the relatively simple – but purposefully designed – geometry, the LDL fans can be manufactured in a relatively cost-effective and quick manner. This fact, together with the fairly good aerodynamic properties, and resistance against solid contaminants, increases the competitiveness of the fan family on the market.

ACKNOWLEDGEMENTS

The authors acknowledge the support by the following organizations and projects. Hungarian National Research, Development and Innovation Centre, under contract No. NKFI K 129023. VEKOP-2.1.7-15-2016-00647 project, supported by the Hungarian Ministry of Finance. The National Talent Programme of the Ministry of Human Capacites, Hungary (NFTO-21-B-0279). The role of Fluid-Lab.Hu Kft. is acknowledged in delivering the CFD data.

REFERENCES

[1] Thakur, P., 2019, *Advanced mine ventilation – Respirable coal dust, combustible gas and mine fire control.* Woodhead Publishing, Duxford, United Kingdom.

[2] U.S. Chemical Safety and Hazard Investigation Board, 2015, US Ink/Sun Chemical Corporation: Ink dust explosion and flash fires in East Rutherford, New Jersey. *Case Study* No. 2013-01-I-NJ. 40 p.

[3] Ghenaiet, A., 2021, Study of particle dynamics and erosion in a centrifugal fan. *Proc. 14th European Conference on Turbomachinery Fluid Dynamics & Thermodynamics ETC14*, April 12-16, 2021; Gdansk, Poland (virtual conference). Paper ID: ETC2021-495. 12 p.

[4] Aldi, N., Casari, N., Pinelli, M., Suman, A., Vulpio, A., Saccenti, P., Beretta, R., Fortini, A., Merlin, M., 2019, Erosion behavior on a large-sized centrifugal fan. *Proc. 13th European Conference on Turbomachinery Fluid Dynamics & Thermodynamics ETC13*, April 8-12, 2019; Lausanne, Switzerland. Paper ID: ETC2019-389. 13 p.

[5] Gruber J. and co-authors, 1978, *Ventilátorok* (*Fans*)(in Hungarian). Műszaki Könyvkiadó, Budapest, Hungary.

[6] The RSES HVACR Training Authority, 2009, Fans and blowers Part I. *Service Application Manual*, SAM Chapter 630-132, Section 11B. 11 p.

[7] Vad, J., Horváth, Cs., Kovács, J. G., 2014, Aerodynamic and aero-acoustic improvement of electric motor cooling equipment. *Proc. Institution of Mechanical Engineers – Part A: Journal of Power and Energy*, **228** (3), pp. 300-316.

[8] *Commission Regulation (EU) No 327/2011* of 30 March 2011 implementing Directive

2009/125/EC of the European Parliament and of the Council with regard to ecodesign requirements for fans driven by motors with an electric input power between 125 *W* and 500 k*W*. Official Journal of the European Union, pp. L90/8-L90/21.

[9] Biedermann, T. M., Moutamassik, Y., Kameier, F., 2022, Assessment of the impeller/volute relationship of centrifugal fans from an aerodynamic and aeroacoustic perspective. *ASME Paper* GT2022-79389.

[10] Vulpio, A., Oliani, S., Suman, A., Zanin, N., Saccenti, P., 2022, A mechanistic model for the predictive maintenance of heavy-duty centrifugal fans operating with dust-laden flows. *ASME Paper* GT2022-82862.

[11] Lukács, E., Vad, J., 2021, Flow topology and loss analysis of a square-to-square sudden expansion relevant to HVAC systems: A case study. *Journal of Building Engineering*, **41**, Paper: 102802, 13 p.

[12] Lukács, E., Vad, J., 2022, A passive loss reduction method of square-to-square sudden expansions. *Energy & Buildings*, **266**, Paper: 112113, 13 p.

[13] Lajos, T., 2015, *Az Áramlástan alapjai* (*Fundamentals of Fluid Mechanics*)(in Hungarian), Vareg Hungary Kft., Budapest, Hungary.

[14] VDI Richtlinien, 1990, *Guideline* VDI 3731 – Blatt 2, Emissionskennwerte technischer Schallquellen, Ventilatoren.

[15] Carolus, T., 2003, *Ventilatoren*, Teubner Verlag, Wiesbaden, Germany.

[16] Osborne, W. C., 1966, *Fans*. Pergamon Press, London, UK.

[17] Wang, J., 2021, Design for high efficiency of low-pressure axial fans: use of blade sweep and vortex distribution. *Ph.D. Thesis*, University of Twente, The Netherlands.

[18] Daly, B. B., 1992, *Woods Practical Guide to Fan Engineering*. Fläkt Woods Ltd. Sixth impression.

[19] Cory, W. T. W., 2005, *Fans & Ventilation – A practical guide*. Elsevier, New York, US.

[20] Fűzy, O., 1991, *Áramlástechnikai gépek és rendszerek* (*Fluid machinery and flow systems*)(in Hungarian). Tankönyvkiadó, Budapest, Hungary.

[21] *International Standard* ISO 5801:2017. Fans - Performance testing using standardized airways.

[22] *International Standard* ISO 5167-1:2003. Measurement of fluid flow by means of pressure differential devices inserted in circular cross-section conduits running full – Part 1: General principles and requirements.

[23] *International Standard* ISO 5167-2:2003. Measurement of fluid flow by means of pressure differential devices inserted in circular cross-section conduits running full – Part 2: Orifice plates.

[24] *International Standard* ISO 13348:2007. Industrial fans – Tolerances, methods of conversion and technical data presentation..

[25] Tóth, D., Vad, J., 2022, Industry 4.0 perspectives of axial and radial fans in smart industrial ventilation: conceptual case studies. *Proc. Conference on Modelling Fluid Flow (CMFF'22)*, 30 August to 02 September 2022, Budapest, Hungary. Paper No.: CMFF22-040.